AIP Applied Physics Letters

Contact to ZnO and intrinsic resistances of individual ZnO nanowires with a circular cross section

Yen-Fu Lin, Wen-Bin Jian, C. P. Wang, Yuen-Wuu Suen, Zhong-Yi Wu, Fu-Rong Chen, Ji-Jung Kai, and Juhn-Jong Lin

Citation: Applied Physics Letters **90**, 223117 (2007); doi: 10.1063/1.2745648
View online: http://dx.doi.org/10.1063/1.2745648
View Table of Contents: http://scitation.aip.org/content/aip/journal/apl/90/22?ver=pdfcov
Published by the AIP Publishing

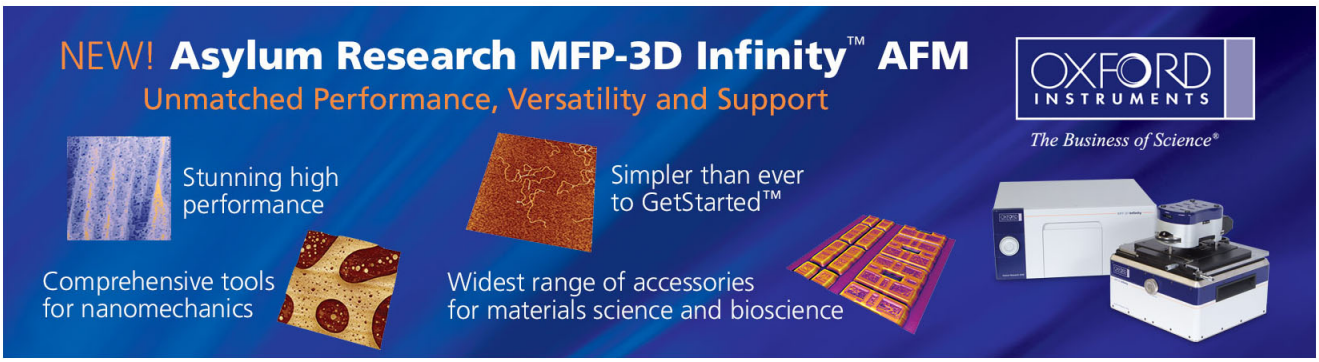

Contact to ZnO and intrinsic resistances of individual ZnO nanowires with a circular cross section

Yen-Fu Lin and Wen-Bin Jian[a)]
Department of Electrophysics, National Chiao Tung University, Hsinchu 30010, Taiwan, Republic of China

C. P. Wang and Yuen-Wuu Suen
Department of Physics, National Chung Hsing University, Taichung 402, Taiwan, Republic of China and National Nano Device Laboratories, Hsinchu 300, Taiwan, Republic of China

Zhong-Yi Wu, Fu-Rong Chen, and Ji-Jung Kai
Department of Engineering and System Science, National Tsing Hua University, Hsinchu 30013, Taiwan, Republic of China

Juhn-Jong Lin
Institute of Physics, National Chiao Tung University, Hsinchu 30010, Taiwan, Republic of China and Department of Electrophysics, National Chiao Tung University, Hsinchu 30010, Taiwan, Republic of China

(Received 19 April 2007; accepted 10 May 2007; published online 1 June 2007)

Single crystalline ZnO nanowires (NWs) with a circular cross section and ~40 nm in diameter have been synthesized and utilized to fabricate two-contact ZnO NW devices. The electrical properties of the NW devices can be categorized into two classes according to the magnitude of their room-temperature resistances. *I-V* curves of low-resistance devices exhibit downward bending features and their temperature dependent resistances demonstrate thermal activation transport in the ZnO NWs. The high-resistance NW devices can be modeled as back-to-back Schottky contacts and the electron transport through the contacts reveals a variable-range-hopping mechanism. © *2007 American Institute of Physics*. [DOI: 10.1063/1.2745648]

Zinc oxide (ZnO) is a direct and wide gap semiconductor with a room-temperature (RT) band gap energy of 3.37 eV.[1] ZnO has a relatively high exciton binding energy of ~60 meV that makes it a suitable material for applications in ultraviolet (UV) laser emission even at RT.[2] Due to oxygen deficiency in this material,[3] ZnO displays native *n*-type conductivity. ZnO can also be heavily doped to form a transparent conductor.[4] Moreover, *p*-type conductivity is realizable,[5] and both Ohmic and Schottky contacts to ZnO are attainable.[6] ZnO attracts much attention due to not only its various applications[7] but also its fascinating and yet-to-be fully understood defect physics.[8]

Recently, by using vapor transport, ZnO has been converted to form quasi-one-dimensional nanowires (NWs).[9] It was then suggested that the NWs may be implemented as building blocks for bottom-up nanotechnology and functional nanoscale electronics.[10] Fabrication and characterization of ZnO NW devices, such as UV photodetectors,[11] gas and chemical sensors,[12,13] field-effect transistors,[14–17] and Schottky diodes[18,19] were demonstrated. In particular, in order to clarify the roles of defects and surface-related conduction, electronic transport properties through individual ZnO NWs have recently been studied by using two-probe[20–24] or four-probe[24] methods. The techniques of the e-beam lithography for electrode fabrication[20–22] and the scanning tunneling microscopy probes for making contacts on ZnO NWs (Refs. 23 and 24) were adopted for current-voltage (*I-V*) characteristic studies.

To fabricate reliable ZnO NW devices, the contacts to ZnO NWs and the intrinsic NW resistance should be understood and controlled. In previous works, conflicting *I-V* characteristics of ZnO NW devices have been reported, which showed either upward or downward bending, or displayed diode behaviors. Meanwhile, measurements of temperature dependent resistances were carried out but discrepant explanations were proposed, including thermally activated transport,[21] thermionic emission model,[16] and the Efros-Shklovskii variable-range hopping.[22] More undesirably, the electrical properties of the contacts and individual ZnO NWs have not been clearly separated. In this work, we fabricated two-contact ZnO NW devices and utilized several devices with negligible contact resistances to determine the intrinsic resistivity of ZnO NWs, and using other devices with high contact resistance to canvass the electrical properties of the contacts to ZnO NWs.

ZnO NWs were synthesized on quartz substrates by thermal evaporation with 40 nm diameter Au nanoparticles as catalysts.[25] The morphology, cross section, and crystalline structures of the NWs were analyzed by using a field-emission scanning electron microscope (FESEM) (JEOL JSM-7000F) and a transmission electron microscope (TEM) (JEOL JEM-2010F). The NWs were dispersed on silicon substrates which were capped with a 400 nm SiO_2 layer and were photolithographically patterned with Au micron electrodes. The standard e-beam lithography technique was used to position individual NWs and to deposit Ti/Au (≈10/100 nm thickness) nanometer-electrodes on them. The two-contact ZnO NW devices were placed in a liquid-nitrogen cryostat and *I-V* curves were measured at various temperatures.

Figure 1(a) exposes the morphology of the as-grown ZnO NWs with lengths of several microns and monodisperse diameter of ~40 nm. The small standard deviation (12%) in the NW diameter largely facilitates the determination of the

[a)]Author to whom correspondence should be addressed; electronic mail: wbjian@mail.nctu.edu.tw

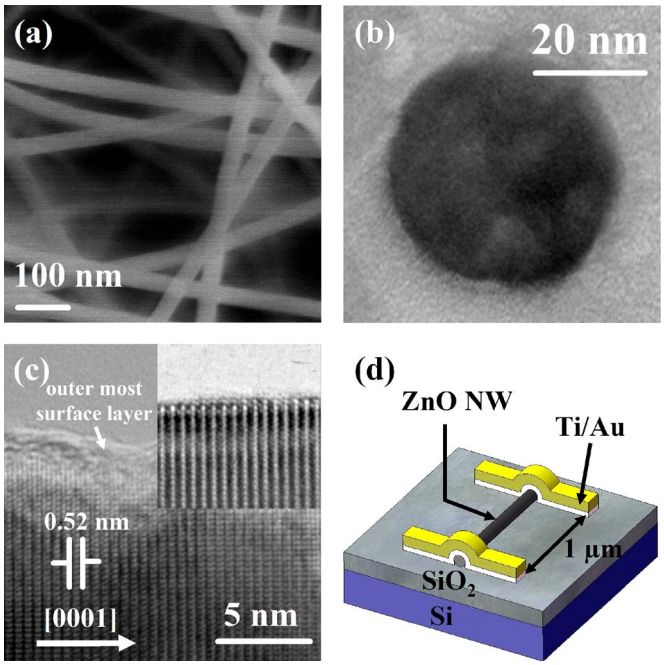

FIG. 1. (Color online) (a) FESEM image of as-grown ZnO NWs. (b) TEM image of a cross section of a single ZnO NW. (c) High-resolution TEM image of an as-grown ZnO NW with lattice spacing, growth direction, and outermost surface layer, as indicated. The inset shows a TEM image of crystalline structure at a boundary surface of a ZnO NW. (d) A schematic diagram illustrating our two-contact ZnO NW devices.

intrinsic resistivity of the NWs. The circular cross section and the single crystalline structure of an as-grown NW are shown in Figs. 1(b) and 1(c), respectively. The high-resolution TEM image reveals the ZnO wurtzite structure with a spacing of 0.52 nm between the (001) planes and the growth direction being along [0001]. The outermost cylindrical surface layer is indicated with an arrow in Fig. 1(c) to delineate that, in some cases, the single crystalline NW could be covered with a noncrystalline or amorphous layer. However, it should be noted that, in other cases, the boundary surface of the ZnO NWs illustrates crystalline structures [see the inset in Fig. 1(c)]. A schematic diagram for our two-contact ZnO NW devices is shown in Fig. 1(d). The separation distance between the two nanometer electrodes is 1 μm in all the NW devices studied in this work.

As just mentioned, the variation in NW diameters is small and the separation distance between the two Ti/Au electrodes is kept constant for all the devices. One might then expect to see similar RT resistances as well as electrical properties in all our NW devices. Surprisingly, we found that the RT resistances ranged from tens to higher than several hundreds of kilohms in the 12 devices studied in this work. In particular, the electrical-transport behaviors can be distinctly categorized into two groups: one with low RT resistances of approximately several tens kilohms and the other with high RT resistance of approximately several hundreds of kilohms.

Figure 2(a) shows the temperature dependent *I-V* curves for a typical ZnO NW device with a low RT resistance. The current rises with the increasing bias voltage and it reveals downward bending characteristics within the limited voltage range of ±1 V. The bending is more profound at lower temperature. The *I-V* curves over a wider voltage range are given in the inset for comparison. On the other hand, the

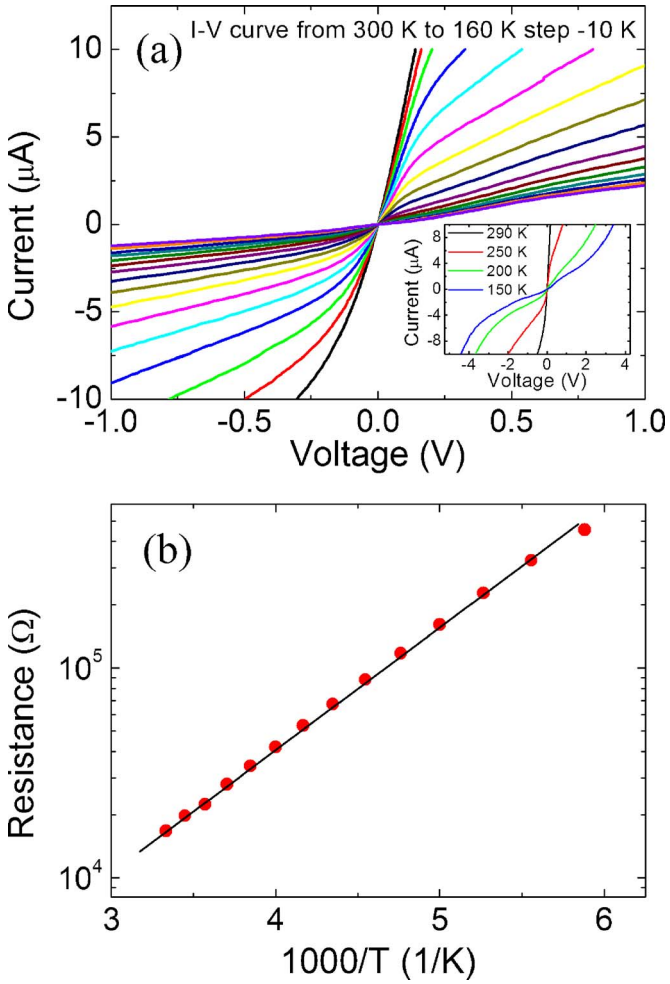

FIG. 2. (Color online) (a) Temperature dependent *I-V* curves of a ZnO NW device with a low RT resistance of 15 kΩ. The temperature range is from 300 (steepest curve) to 160 K (flattest curve). *I-V* curves in wider voltage range are plotted in the inset. (b) Resistance of the NW device as a function of inverse temperature.

temperature dependent resistance, $R(T)$, [Fig. 2(b)] reveals a linear variation of $\ln R$ with $1/T$, which conforms to the thermally activated transport given by $R=R_0 \exp(E_a/k_BT)$, where k_B is the Boltzmann constant and E_a is the activation energy. In connection with the fact of a low RT resistance, we propose that the two-contact NW devices can provide a faithful measurement of the intrinsic resistivity of individual ZnO NWs. Assuming negligible contact resistances, we found an average intrinsic resistivity of a few $m\Omega$ cm from six low RT resistance NW devices, which is in line with the value obtained from our four-probe measurements (not shown). The average activation energy E_a is ≈100 meV and could be attributed to shallow donors of native defects in ZnO.[8,21]

The second group of ZnO NW devices with high RT resistances displays upward bending features in *I-V* curves [Fig. 3(a)] over the entire voltage range. Because the RT resistances in this case are more than one order of magnitude higher than those in the low RT resistance devices, we believe that the contact resistances dominate in these high-resistance NW devices. The inset in Fig. 3(a) indicates that $\ln(I/T^2)$ varies linearly with $1/T$, which well fits to the thermionic emission theory in reverse bias given by the form $I=aA^{**}T^2 \exp(-q\phi_B/k_BT)$,[26] where a is the contact area, A^{**}

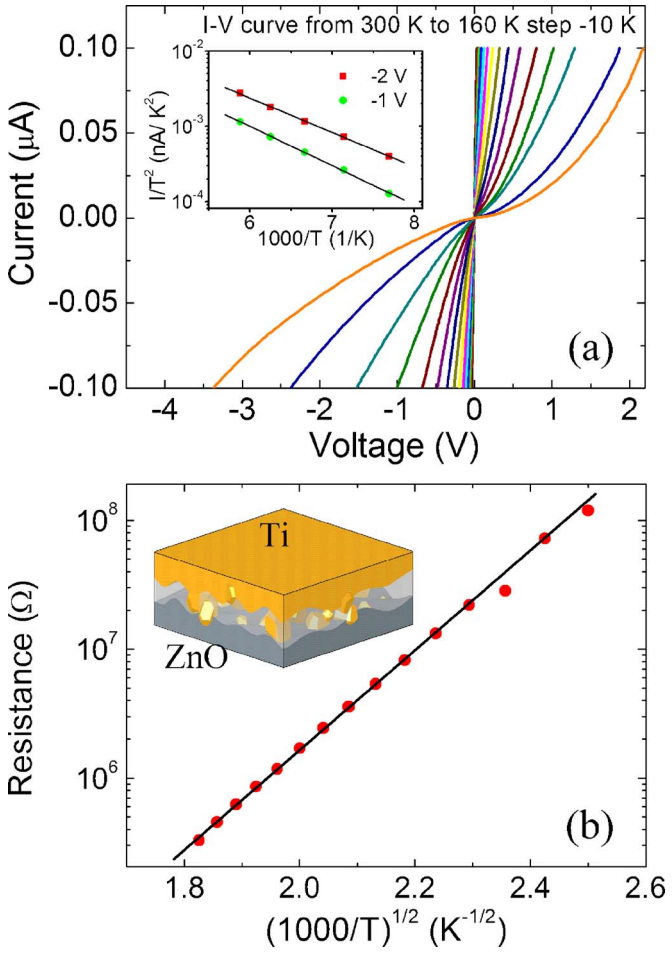

FIG. 3. (Color online) (a) *I-V* curves of a ZnO NW device with a high RT resistance of 350 kΩ. Inset: I/T^2 as a function of inverse temperature. (b) Resistance of the NW device as a function of $T^{-1/2}$. The inset schematically depicts the contact between Ti electrode and ZnO NW.

is the effective Richardson constant, and $q\phi_B$ is the barrier height. Thus, the back-to-back Schottky contact model adequately describes our (six) high-resistance devices, with an average $q\phi_B \sim 100$ meV. As shown in Fig. 3(b), the temperature dependent resistance, in sharp contrast to thermally activated transport, displays a variable range hopping mechanism of the form $R=A\exp(BT^{-1/2})$,[27] where A and B are constants. Knowing that some ZnO NWs comprised noncrystalline surfaces [Fig. 1(c)], we can possibly envisage the electrical transport behavior in this case to be governed by electron hopping through a nonconducting layer formed between the Ti/Au electrodes and the ZnO NW, as is schematically depicted in the inset of Fig. 3(b).

In summary, the ZnO NW devices can be categorized into two classes according to their RT resistances. The low RT resistance devices may be used to determine the intrinsic resistivity of individual ZnO NWs. The *I-V* curves of these devices exhibit downward bending features and their temperature dependent resistances reveal thermal activation transport. In high RT resistance devices, the *I-V* curves display upward bending characteristics all over the voltage range and can be fitted to the thermionic emission theory. The temperature dependent resistance is due to variable-range hopping of electrons through the contacts.

This work was supported by the Taiwan National Science Council under Grant Nos. NSC 94-2112-M-009-020, NSC 94-2120-M-009-010, and NSC 95-2120-M-009-002, and by the MOE ATU Program.

[1] D. M. Bagnall, Y. F. Chen, Z. Zhu, T. Yao, S. Koyama, M. Y. Shen, and T. Goto, Appl. Phys. Lett. **70**, 2230 (1997).
[2] Z. K. Tang, G. K. L. Wong, P. Yu, M. Kawasaki, A. Ohtomo, H. Koinuma, and Y. Segawa, Appl. Phys. Lett. **72**, 3270 (1998).
[3] A. Tiwari, C. Jin, J. Narayan, and M. Park, J. Appl. Phys. **96**, 3827 (2004).
[4] Y. W. Heo, S. J. Park, K. Ip, S. J. Pearton, and D. P. Norton, Appl. Phys. Lett. **83**, 1128 (2003).
[5] S. Kim, B. S. Kang, F. Ren, Y. W. Heo, K. Ip, D. P. Norton, and S. J. Pearton, Appl. Phys. Lett. **84**, 1904 (2004).
[6] K. Ip, G. T. Thaler, H. Yang, S. Y. Han, Y. Li, D. P. Norton, S. J. Pearton, S. Jang, and F. Ren, J. Cryst. Growth **287**, 149 (2006).
[7] S. J. Pearton, D. P. Norton, K. Ip, Y. W. Heo, and T. Steiner, J. Vac. Sci. Technol. B **22**, 932 (2004).
[8] S. B. Zhang, S.-H. Wei, and A. Zunger, Phys. Rev. B **63**, 075205 (2001).
[9] M. H. Huang, Y. Wu, H. Feick, N. Tran, E. Weber, and P. Yang, Adv. Mater. (Weinheim, Ger.) **13**, 113 (2001).
[10] X. Duan, Y. Huang, Y. Chi, J. Wang, and C. M. Lieber, Nature (London) **409**, 66 (2001).
[11] H. Kind, H. Yan, B. Messer, M. Law, and P. Yang, Adv. Mater. (Weinheim, Ger.) **14**, 158 (2002).
[12] Q. H. Li, Y. X. Liang, Q. Wan, and T. H. Wang, Appl. Phys. Lett. **85**, 6389 (2004).
[13] Z. Fan and J. G. Lu, Appl. Phys. Lett. **86**, 123510 (2005).
[14] Y. W. Heo, L. C. Tien, Y. Kwon, D. P. Norton, S. J. Pearton, B. S. Kang, and F. Ren, Appl. Phys. Lett. **85**, 2274 (2004).
[15] W. I. Park, J. S. Kim, G. C. Yi, M. H. Bae, and H.-J. Lee, Appl. Phys. Lett. **85**, 5052 (2004).
[16] Z. Fan, D. Wang, P. C. Chang, W. Y. Tseng, and J. G. Lu, Appl. Phys. Lett. **85**, 5923 (2004).
[17] S. Ju, K. Lee, D. B. Janes, M. H. Yoon, A. Facchetti, and T. J. Marks, Nano Lett. **5**, 2281 (2005).
[18] Y. W. Heo, L. C. Tien, D. P. Norton, S. J. Pearton, B. S. Kang, F. Ren, and J. R. LaRoche, Appl. Phys. Lett. **85**, 3107 (2004).
[19] C. S. Lao, J. Liu, P. Gao, L. Zhang, D. Davidovic, R. Tummala, and Z. L. Wang, Nano Lett. **6**, 263 (2006).
[20] Q. H. Li, Q. Wan, Y. X. Liang, and T. H. Wang, Appl. Phys. Lett. **84**, 4556 (2004).
[21] Y. W. Heo, L. C. Tien, D. P. Norton, B. S. Kang, F. Ren, G. P. Gila, and S. J. Pearton, Appl. Phys. Lett. **85**, 2002 (2004).
[22] Y. J. Ma, Z. Zhang, F. Zhou, L. Lu, A. Jin, and C. Gu, Nanotechnology **16**, 746 (2005).
[23] Z. Y. Zhang, C. H. Jin, X. L. Liang, Q. Chen, and L.-M. Peng, Appl. Phys. Lett. **88**, 073102 (2006).
[24] X. Lin, X. B. He, T. Z. Yang, W. Guo, D. X. Shi, H.-J. Gao, D. D. D. Ma, S. T. Lee, F. Liu, and X. C. Xie, Appl. Phys. Lett. **89**, 043103 (2006).
[25] Z. Y. Wu, F. R. Chen, J. J. Kai, W. B. Jian, and J. J. Lin, Nanotechnology **17**, 5511 (2006).
[26] S. M. Sze, *Physics of Semiconductor Devices*, 2nd ed. (Wiley, New York, 1981), p. 258.
[27] N. F. Mott and E. A. Davis, *Electronic Processes in Non-Crystalline Materials*, 2nd ed. (Clarendon, Oxford, 1979), p. 34.